

# Using Micromachining, Molecular Self-Assembly, and Wet Etching to Fabricate 0.1-1- $\mu$ m-Scale Structures of Gold and Silicon

Nicholas L. Abbott, Amit Kumar, and George M. Whitesides\*

Department of Chemistry, Harvard University, Cambridge, Massachusetts 02138

Received September 14, 1993. Revised Manuscript Received February 2, 1994\*

A combination of molecular self-assembly and micromachining was used to pattern the surface of thin films of gold with 0.1-1- $\mu$ m-sized regions of monolayers formed from HO(CH<sub>2</sub>)<sub>2</sub>SH and CH<sub>3</sub>(CH<sub>2</sub>)<sub>15</sub>SH. Selective, wet chemical etching of gold supporting patterned, self-assembled monolayers resulted in the formation of microstructures of gold on substrates of silicon or glass. Using this procedure, it is possible to construct electrically conducting wires of gold with cross sections as small as 200 nm  $\times$  25 nm and lengths  $\geq$  15  $\mu$ m. Complex and closely spaced microstructures, such as parallel and collinear wires separated by  $<$  1  $\mu$ m, can also be fabricated. Microstructures of gold served as masks for wet etching of silicon (aqueous solutions of 2 M KOH) and were used to form multilayer structures of gold and silicon. This method of microfabrication is a simple one, can be performed in any wet chemical laboratory, and, we believe, can be scaled to smaller dimensions.

## Introduction

In this paper, we report a procedure that combines micromachining,<sup>1</sup> molecular self-assembly, and wet etching and provides the basis for a method to fabricate 0.1-1- $\mu$ m-scale structures of gold supported on glass or silicon. This procedure has four steps: (i) formation of a monolayer of the thiolate<sup>2</sup> [HO(CH<sub>2</sub>)<sub>2</sub>S] from  $\beta$ -mercaptoethanol [HO(CH<sub>2</sub>)<sub>2</sub>SH] on the surface of a film of gold; (ii) generation, by micromachining, of 0.1-1- $\mu$ m-scale regions of bare gold in the monolayer of HO(CH<sub>2</sub>)<sub>2</sub>S; (iii) self-assembly of a monolayer of CH<sub>3</sub>(CH<sub>2</sub>)<sub>15</sub>S on micromachined regions of bare gold;<sup>3</sup> (iv) selective etching of gold film underlying HO(CH<sub>2</sub>)<sub>2</sub>S by using an aqueous solution of cyanide ions (CN<sup>-</sup>) saturated with O<sub>2</sub>. Areas of gold film supporting self-assembled monolayers (SAMs) of CH<sub>3</sub>(CH<sub>2</sub>)<sub>15</sub>S are protected from etching<sup>4</sup> and form microstructures of gold with lateral dimensions as small as 0.1  $\mu$ m and vertical dimensions as small as 25 nm.<sup>5</sup>

Because gold is a good electrical conductor and does not oxidize in air, it is frequently used in the fabrication of small structures. Microstructures of gold are used as microelectrodes,<sup>6</sup> small conductors for dense microelectronic devices,<sup>7</sup> scatterers and absorbers for ion projection lithography and etching,<sup>7,8</sup> and masks for X-ray lithography.<sup>7,9</sup> Here we report a simple, wet chemical procedure for fabricating 0.1-1- $\mu$ m-scale structures of gold. In

contrast to conventional techniques of microfabrication, this procedure does not require access to high-vacuum equipment or the fabrication of photolithographic masks<sup>10</sup> and is, therefore, well-suited for the prototyping of microstructures. This procedure can, in addition, be performed on radiation sensitive substrates or substrates with complex geometries and can, in principle, be scaled to dimensions not accessible by conventional techniques of microfabrication. By using atomic force microscopy (AFM) and scanning tunneling microscopy (STM) to micromachine organic monolayers supported on gold films, this procedure can be scaled, we believe, to dimensions  $<$  10 nm.

Self-assembled monolayers (SAMs) of organic molecules formed on the surface of gold (and on other metals: Ag, Cu, and Ni) have been used extensively in the study of the physical chemistry of organic interfaces.<sup>11-15</sup> We used SAMs of alkanethiolates, formed by the reaction of

\* Abstract published in *Advance ACS Abstracts*, March 15, 1994.

(1) We use the term "micromachining" to mean the moving of metal by mechanical means rather than by chemical etching.

(2) The composition of the surface is probably a mixture of HO(CH<sub>2</sub>)<sub>2</sub>SAu and HO(CH<sub>2</sub>)<sub>2</sub>S(Au)<sub>3</sub>. For simplicity, we denote the species bound to the surface as HO(CH<sub>2</sub>)<sub>2</sub>S.

(3) Abbott, N. L.; Folkers, J. P.; Whitesides, G. M. *Science* 1992, 257, 1380.

(4) Kumar, A.; Biebuyck, H. A.; Abbott, N. L.; Whitesides, G. M. *J. Am. Chem. Soc.* 1992, 114, 9188.

(5) The vertical dimension of the microstructure is determined by the thickness of the gold film.

(6) Bond, A. M.; Henderson, T. L. E.; Thormann, W. *J. Phys. Chem.* 1986, 90, 2911. Abe, T.; Itaya, K.; Uchida, I. *Chem. Lett.* 1988, 399. Thormann, W.; van den Bosch, P.; Bond, A. M. *Anal. Chem.* 1985, 57, 2764. Samuelsson, M.; Armgarth, M.; Nylander, C. *Anal. Chem.* 1991, 63, 931. Wightman, R. M. *Science (Washington D.C.)* 1988, 240, 415 and references therein.

(7) Brodie, I.; Muray, J. J. *The Physics of Micro/Nano-Fabrication*; Plenum: New York, 1992, and references therein.

(8) Bartlet, J. L.; Slayman, C. W.; Wood, J. E.; Cheyn, J. Y.; McKenna, C. M. *J. Vac. Sci. Technol.* 1981, 19, 1166.

(9) Chiu, S. L.; Acosta, R. E. *J. Vac. Sci. Technol. B* 1990, 8, 1589. Kebabi, B.; Malek, C. K. *J. Vac. Sci. Technol. B* 1991, 9, 154.

(10) Bruning, J. *Opt. Photonics News* 1991, 2, 23.

(11) Formation: Nuzzo, R. G.; Allara, D. L. *J. Am. Chem. Soc.* 1983, 105, 4481. Nuzzo, R. G.; Fusco, F. A.; Allara, D. L. *J. Am. Chem. Soc.* 1987, 109, 2358. Bain, C. D.; Troughton, E. B.; Tao, Y.-T.; Evall, J.; Whitesides, G. M.; Nuzzo, R. G. *J. Am. Chem. Soc.* 1989, 111, 321. Whitesides, G. M.; Laibinis, P. E. *Langmuir* 1990, 6, 87 and references therein.

(12) Wetting: Bain, C. D.; Whitesides, G. M. *J. Am. Chem. Soc.* 1988, 110, 5897. Bain, C. D.; Whitesides, G. M. *Langmuir* 1989, 5, 1370. Dubois, L. H.; Zegarski, B. R.; Nuzzo, R. G. *J. Am. Chem. Soc.* 1990, 112, 570. Laibinis, P. E.; Whitesides, G. M. *J. Am. Chem. Soc.* 1992, 114, 1990.

(13) Adhesion: Allara, D. L.; Hebard, A. F.; Padden, F. J.; Nuzzo, R. G.; Falcone, D. R. *J. Vac. Sci. Technol. A* 1983, 376. Stewart, K. R.; Whitesides, G. M.; Godfried, H. P.; Silvera, I. F. *Rev. Sci. Instrum.* 1986, 57, 1381. Czanderna, A. W.; King, D. E.; Spaulding, D. *J. Vac. Sci. Technol. A* 1991, 9, 2607. Armstrong, F. A.; Hill, H. A. O.; Walton, N. J. *Acc. Chem. Res.* 1988, 21, 407. Pale-Grosemange, C.; Simon, E. S.; Prime, K. L.; Whitesides, G. M. *J. Am. Chem. Soc.* 1991, 113, 12. Haussling, L.; Michel, B.; Ringsdorf, H.; Rohrer, H. *Angew. Chem., Int. Ed. Engl.* 1991, 30, 569. Tarlov, M. J.; Bowden, E. F. *J. Am. Chem. Soc.* 1991, 113, 1847. Prime, K. L.; Whitesides, G. M. *Science (Washington, D.C.)* 1991, 252, 1164. Haussling, L.; Ringsdorf, H.; Schmitt, F.-J.; Knoll, W. *Langmuir* 1991, 7, 1837.

alkanethiols with the surface of gold, because (i) monolayers of  $\text{HO}(\text{CH}_2)_2\text{S}$  can be mechanically removed to expose 0.1–1- $\mu\text{m}$ -scale regions of underlying gold, (ii) the chemisorption of organosulfur compounds on the surface of gold is selective—machined regions of bare gold can be functionalized with  $\text{CH}_3(\text{CH}_2)_{15}\text{S}$  without completely displacing  $\text{HO}(\text{CH}_2)_2\text{S}$  from the surrounding surface of the gold film, and (iii) the physical properties of a gold film can be controlled by the structure of the chemisorbed molecules—films of gold-supporting monolayers of  $\text{HO}(\text{CH}_2)_2\text{S}$  are etched by aqueous solutions of cyanide ions saturated with  $\text{O}_2$ : SAMs of  $\text{CH}_3(\text{CH}_2)_{15}\text{S}$ , in contrast, protect an underlying film of gold from etching. We have found that the ability of a monolayer to passivate a surface of gold to etching by aqueous solutions of  $\text{CN}^-$  saturated with  $\text{O}_2$  appears to be a combined effect of the thickness of a monolayer and its hydrophilicity: monolayers formed from alkanethiols terminated in polar groups ( $-\text{OH}$ ,  $-\text{COOH}$ ) afford less protection to the surface as compared to the methyl-terminated alkanethiols of equivalent length.

We have demonstrated the capability of micromachining, molecular self-assembly, and wet chemical etching to fabricate microstructures having a variety of geometries. Electrically conducting wires of gold were fabricated with cross sections as small as  $200\text{ nm} \times 25\text{ nm}$  and lengths  $\geq 15\ \mu\text{m}$ . Four-probe conductivity measurements at room temperature showed that these microwires were electrically conducting with resistivities similar to bulk gold. Gold microstructures on silicon were also used as masks for an anisotropic etchant of silicon (aqueous solutions of 2 M KOH): micrometer-scale relief structures of silicon, as well as multilayer structures of gold and silicon, were fabricated. We also prepared closely spaced microstructures of gold from (i) parallel wires of gold that were separated by  $\sim 0.5\ \mu\text{m}$  over lengths  $> 100\ \mu\text{m}$  and (ii) collinear wires of gold that were separated from each other by 0.7- $\mu\text{m}$ -wide, electrically insulating gaps.

The procedure reported here for forming microstructures for gold contrasts to previous work in which micromachining, self-assembled monolayers, and wet chemical etching were used to fabricate “negative” features (trenches) in films of gold.<sup>4</sup>

### Fabrication of Microstructures

Figure 1 is a schematic illustration of the procedure used to fabricate microstructures of gold supported on silicon or glass. The process began with the patterning of a gold film with well-defined areas formed from monolayers of either  $\text{HO}(\text{CH}_2)_2\text{S}$  or  $\text{CH}_3(\text{CH}_2)_{15}\text{S}$ .<sup>3</sup> First, a monolayer of  $\text{HO}(\text{CH}_2)_2\text{S}$  was chemisorbed on the surface of the gold by immersing it in an ethanolic solution of  $\text{HO}(\text{CH}_2)_2\text{SH}$  (Figure 1a). Second, 0.1–1- $\mu\text{m}$ -wide grooves of bare gold were micromachined into the monolayer of  $\text{HO}(\text{CH}_2)_2\text{S}$  using the tip of surgical scalpel blade or the cut end of a

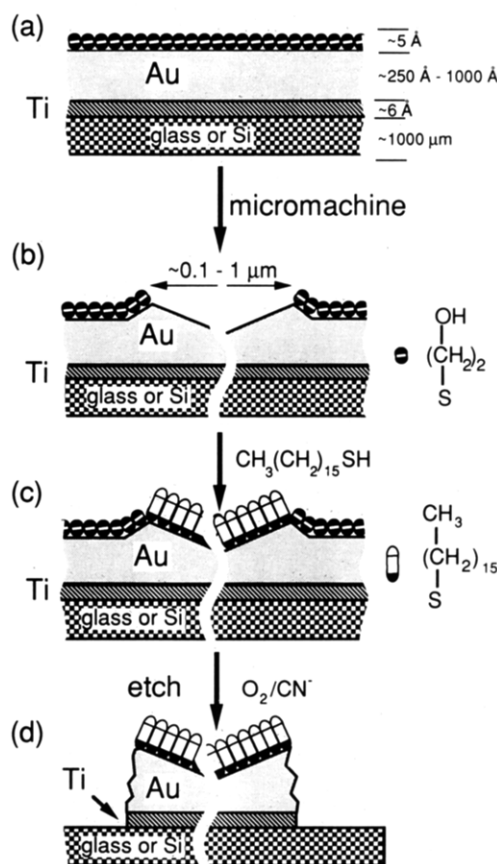


**Figure 1.** Schematic illustration of the procedure used to form 0.1–1- $\mu\text{m}$ -scale structures of gold supported on glass: (a) a monolayer of  $\text{HO}(\text{CH}_2)_2\text{S}$  was chemisorbed on the surface of a gold film; (b) 0.1–1- $\mu\text{m}$ -wide grooves of bare gold were micromachined into the monolayer of  $\text{HO}(\text{CH}_2)_2\text{S}$ ; (c) a SAM of  $\text{CH}_3(\text{CH}_2)_{15}\text{S}$  was formed selectively on the micromachined regions of bare gold; (d) areas of gold film covered with  $\text{HO}(\text{CH}_2)_2\text{S}$  were selectively etched in an aqueous solution of  $\text{CN}^-$  that was sparged with  $\text{O}_2$ : the areas of gold film covered with SAMs of  $\text{CH}_3(\text{CH}_2)_{15}\text{S}$  were protected from the etchant. Titanium (Ti) was used to promote the adhesion between the glass (or silicon) substrate and the film of gold. The illustration is not drawn to scale.

carbon fiber (Figure 1b). The dimensions of the micromachined regions of bare gold were influenced by both the shape of the machining tip and the size of the mechanical load applied to the tip. Figures 2a,b show scanning electron micrographs (SEMs) of the tip of a surgical scalpel blade. A diagram of the apparatus used to control both the position of the tip of the blade and the mechanical load on the tip is shown in Figure 2c. The scalpel blade was hung between a pair of tweezers that were mounted over an X–Y translation stage. The combined weight of the scalpel blade and attached paper clips maintained a constant load ( $\sim 3\text{ mN}$ ) on the tip during machining. The tip of the scalpel blade was translated across the film of gold at a rate of  $\sim 1\text{ mm/s}$ : this procedure produced grooves with continuous, uniform, and reproducible dimensions ( $\sim 1\ \mu\text{m}$  in width). Cross-sectional profiles of the grooves<sup>3</sup> show depths of  $\sim 0.05\ \mu\text{m}$  and raised edges ( $\sim 0.1\ \mu\text{m}$  high and  $\sim 0.2\ \mu\text{m}$  wide) formed by the plastic deformation of the gold during micromachining. Figure 3a,b shows SEMs of the end of a carbon fiber (10  $\mu\text{m}$  in diameter) that was cut using scissors. The shape of each tip varied from cut to cut, and these variations were reflected in the dimensions of the micromachined grooves. Typically, however, grooves with lateral dimensions of  $\sim 0.1\ \mu\text{m}$  were produced using the carbon

(14) X-ray Induced Damage: Bain, C. D. Ph.D. Thesis, Harvard University, 1988. Laibinis, P. E.; Graham, R. L.; Biebuyck, H. A.; Whitesides, G. M. *Science (Washington, D.C.)* 1991, 254, 981.

(15) Electron Transfer: Sabatani, E.; Rubinstein, I. *J. Phys. Chem.* 1987, 91, 6663. (b) Porter, M. D.; Bright, T. B.; Allara, D. L.; Chidsey, C. E. D. *J. Am. Chem. Soc.* 1987, 109, 3559. Chidsey, C. E. D.; Loiacono, D. N. *Langmuir* 1990, 6, 682. Chidsey, C. E. D.; Bertozzi, C. R.; Putvinski, T. M. *J. Am. Chem. Soc.* 1991, 112, 4301. Miller, C.; Cuendet, P.; Gratzel, M. *J. Phys. Chem.* 1991, 95, 877. Hickman, J. J.; Ofer, D.; Zou, C. F.; Wrighton, M. S.; Laibinis, P. E.; Whitesides, G. M. *J. Am. Chem. Soc.* 1991, 113, 1128. Miller, C.; Gratzel, M. *J. Phys. Chem.* 1991, 95, 919. Finklea, H. O.; Hanshew, D. D. *J. Am. Chem. Soc.* 1992, 114, 3175 and references therein.

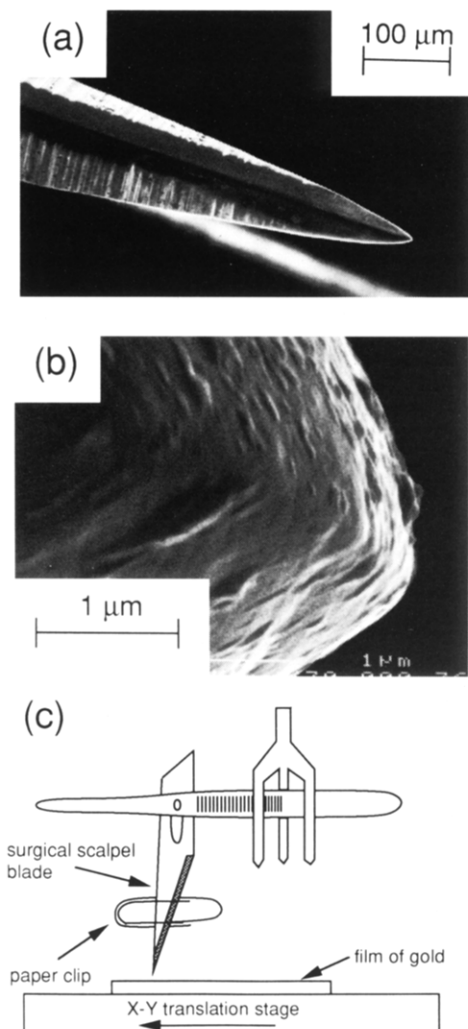


**Figure 2.** Scanning electron micrographs (a and b) of the tip of a surgical scalpel blade used to micromachine gold film supporting self-assembled monolayers of organic molecules. Figure 2c is a schematic illustration of the apparatus used to position the blade and control the machining pressure: the blade was hung between a pair of tweezers that were mounted over an X-Y translation stage. The combined weight of the blade and attached paper clips maintained a constant load ( $\sim 3$  mN) on the tip during machining.

fiber as a machining tool.<sup>16</sup> For ease of manipulation, each carbon fiber was mounted in a block of epoxy resin. The mounted carbon fiber was positioned over an X-Y translation stage, and the load on the machining tip was controlled by using the length of the fiber ( $\sim 10$  mm) as a cantilever (Figure 3c). The third and final step in the patterning of the surface of the gold film is illustrated in Figure 1c: a SAM of  $\text{CH}_3(\text{CH}_2)_{15}\text{S}$  was formed selectively on the micromachined regions of bare gold by immersing the sample in an ethanolic solution of  $\text{CH}_3(\text{CH}_2)_{15}\text{S}$  for 10 s.<sup>17</sup>

The patterns formed by monolayers of  $\text{HO}(\text{CH}_2)_2\text{S}$  and  $\text{CH}_3(\text{CH}_2)_{15}\text{S}$  on the surface of the gold film were transferred into the gold film by wet chemical etching. The areas of gold film covered with  $\text{HO}(\text{CH}_2)_2\text{S}$  were selectively

(16) The cut ends of the carbon fibers sometimes formed distinct parallel grooves in the gold. The grooves were typically separated by 0.1–0.5 μm.

(17) Immersion times longer than  $\sim 30$  s resulted in partial displacement of  $\text{HO}(\text{CH}_2)_2\text{S}$  by  $\text{CH}_3(\text{CH}_2)_{15}\text{S}$  on the surface of the gold. Accompanying the displacement reaction was an increase in the time required to etch the gold film covered initially with  $\text{HO}(\text{CH}_2)_2\text{S}$ .

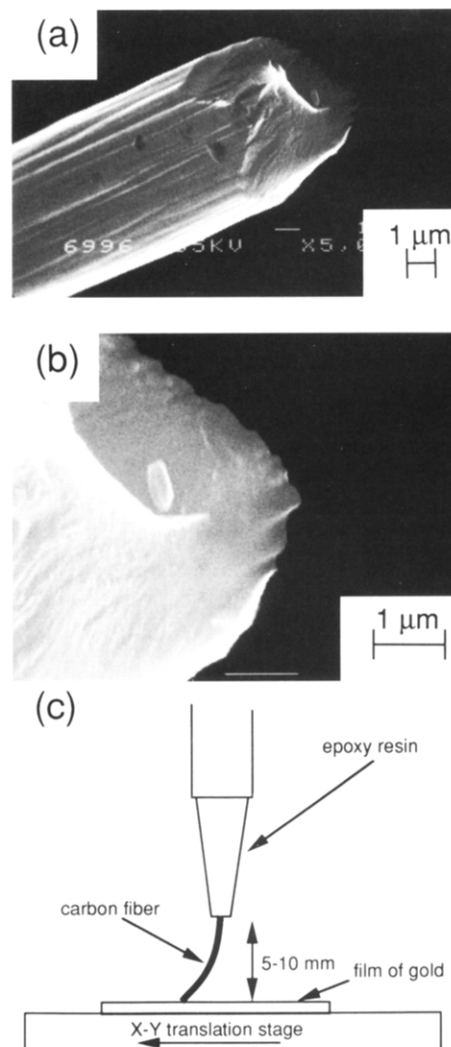


**Figure 3.** Scanning electron micrographs (a and b) of the cut end of a carbon fiber with a diameter of 10 μm. The size and shape of the micromachined grooves are probably determined by local features on the tip of the carbon fiber. Figure 3c is a schematic illustration of the apparatus used to position the carbon fiber and control the machining pressure on the tip. The fiber was positioned over an X-Y translation stage and the load on the machining tip was controlled by using the length of the fiber ( $\sim 10$  mm) as a cantilever.

etched in an aqueous solution of 1 M KOH and 0.1 M KCN that was sparged with  $\text{O}_2$  and vigorously stirred: the areas of the gold film covered with SAMs formed from  $\text{CH}_3(\text{CH}_2)_{15}\text{S}$  were protected from the etchant.<sup>4</sup> The protection of the film of gold appeared to be influenced by both the thickness of the monolayers and its hydrophobicity. For example, 250-Å-thick films of gold supporting monolayers of  $\text{HO}(\text{CH}_2)_2\text{S}$  etched in 5–10 min and 1000-Å-thick gold films etched in  $\sim 45$ –60 min. In contrast, the time to etch gold films covered with a monolayer formed from  $\text{CH}_3(\text{CH}_2)_{15}\text{S}$  was 30 min (250 Å) and 90 min (1000 Å). Because an aqueous solution of  $\text{CN}^-/\text{O}_2$  is an isotropic etchant of gold, the lateral resolution of the etching process was influenced, in part, by the thickness of the gold film. To minimize undercutting of the SAM during etching of the gold, we maintained the ratio of the thickness of the gold film ( $t$ ) and the minimum lateral dimension of the microstructure ( $d$ ) less than 4 ( $t/d < 4$ ).

Control experiments were performed in which monolayers of  $\text{HO}(\text{CH}_2)_2\text{S}$  were formed on the micromachined regions of gold and then etched with aqueous  $\text{CN}^-/\text{O}_2$ .

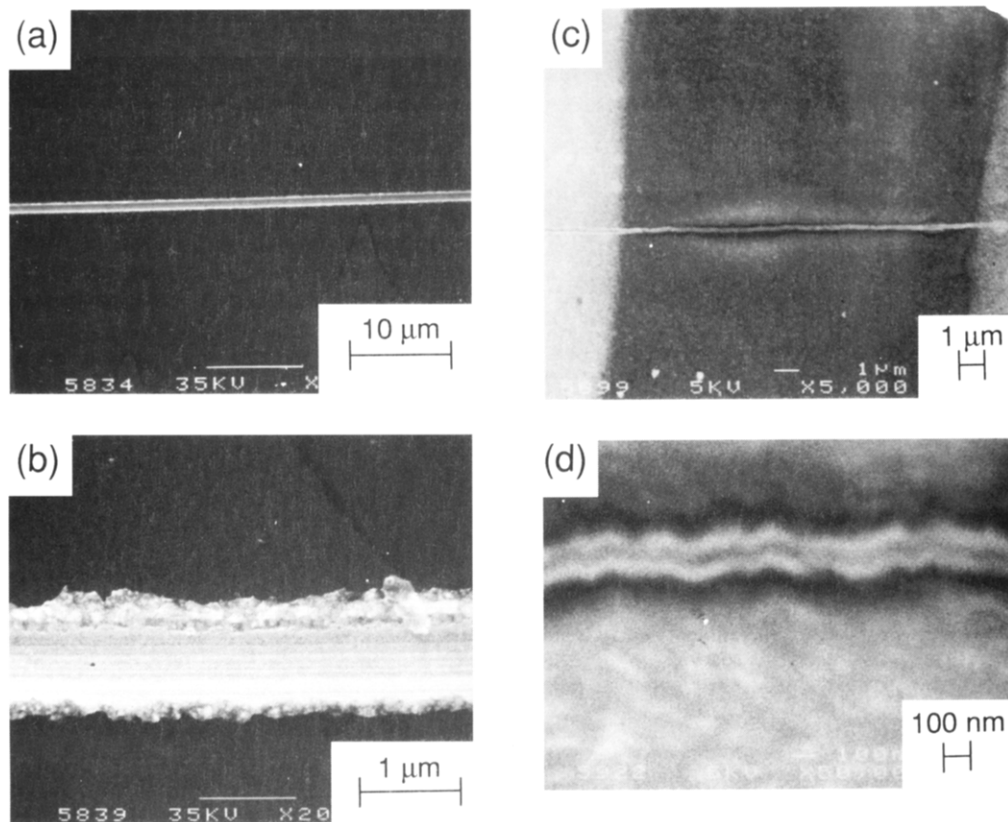


**Figure 4.** Scanning electron micrographs (a and b) of 1- $\mu\text{m}$ -wide, 100-nm-thick wires of gold supported on glass (top view). Wires of this type were uniform in width over lengths exceeding 800  $\mu\text{m}$ . The sample was sputter-coated with  $\sim 50$  Å of gold to suppress charging of the glass substrate during imaging; the accelerating voltage of the electrons was 35 kV. Micrographs (c) and (d) are of a 200-nm-wide, 25-nm-thick, electrically conducting wire of gold that connected two electrical contact pads of gold. The contact pads are the light areas on the left and right sides of the SEM in (c). Because the image of the wire had to be obtained before the resistance was measured (and the wire was severed; see text for details), the wire and glass substrate could not be sputter-coated with gold to suppress the charging of the glass substrate. An accelerating voltage of 5 kV was used to minimize the charging of the glass and yet maintain sufficient signal to obtain images with a resolution better than 200 nm.

This procedure did not result in the formation of microstructures of gold: the micromachined regions were etched at a rate similar (slightly slower<sup>18</sup>) to the surrounding film of gold covered with  $\text{HO}(\text{CH}_2)_2\text{S}$ .

Other details of the experimental procedure can be found in the Experimental Section.

### Results

Figure 4a,b shows SEMs of 1  $\mu\text{m}$  wide  $\times$  100 nm thick wires of gold supported on glass. These wires, which were uniform in width ( $1 \pm 0.2 \mu\text{m}$ ) over lengths ranging from 400 to 800  $\mu\text{m}$ , were fabricated by micromachining with a  $\sim 3$ -mN load applied to the tip of a surgical scalpel. Three wires of the type shown in Figure 4a,b were fabricated between two macroscopic areas of gold film ( $\sim 1 \text{ cm} \times \sim 1 \text{ cm}$ ) that served as electrical contact pads. The contact pads were used to measure the electrical resistance of the wires and were prepared prior to the fabrication of the wires by dipping both ends of a gold film in neat  $\text{CH}_3(\text{CH}_2)_{15}\text{SH}$ . A 400–800- $\mu\text{m}$ -wide area of bare gold was left in the middle of the gold film on which the wires were prepared.

(18) A film of 1000 Å of gold supported on glass and covered with  $\text{HO}(\text{CH}_2)_2\text{S}$  was etched to transparency in 60 min. Micromachined grooves of gold covered with  $\text{HO}(\text{CH}_2)_2\text{S}$  were visible by optical microscopy after 60 min of etching; they were not visible, however, after a total of 75 min of etching. The difference in the rates of etching may be caused by the transfer of material (metal or organics coatings on the scalpel) from the tip of the scalpel to the surface of the gold during micromachining.

We measured the combined resistance of the three parallel wires using four osmium probes (spacing 1.6 mm; radii 0.13 mm). Electrical contact was made by pressing the probes against the surface of the gold contact pads with a force of 40–70 g (0.4–0.7 N). Conductivity measurements were performed with a constant current of 1 mA and at room temperature. After measurement of the combined resistance of the three wires, one of the wires was cut using a diamond knife, and then the resistance of the remaining two wires was measured. This procedure was repeated twice, at which point all three wires were severed. The open-circuit resistance (with three severed wires) was measured to be  $>20 \text{ M}\Omega$ . Using this technique, the resistance (length) of each gold wire was measured to be 116  $\Omega$  (370  $\mu\text{m}$ ), 183  $\Omega$  (584  $\mu\text{m}$ ), and 209  $\Omega$  (775  $\mu\text{m}$ ).

We calculated the resistivity of gold in the wires using the measured resistances and eq 1, where  $r$  is the resistivity

$$r = Rtw/L \quad (1)$$

of gold in the wire ( $\Omega \text{ cm}$ ),  $R$  is the resistance (ohms),  $t$  is the thickness (centimeters),  $w$  is the width (centimeters) and  $L$  is the length of the wire (centimeters). By assuming the thickness of the wire to be 100 nm (corresponding to the thickness of the gold film), the resistivity of gold in a 1  $\mu\text{m}$  wide  $\times$  100 nm thick wire was estimated using eq 1 to be  $(3.0 \pm 0.03) \times 10^{-6} \Omega \text{ cm}$ : this estimate is close to that of bulk gold ( $2.44 \times 10^{-6} \Omega \text{ cm}$ ).<sup>19</sup> The difference between the two values may arise from the assumption

that the thickness of the wire was 100 nm: the process of micromachining probably causes the thickness of the wire (at the center of the wire and edges, at least) to be less than that of the gold film from which the wire was fabricated.

Figure 4c,d shows SEMs of a 200 nm wide  $\times$  25 nm thick  $\times$  15  $\mu\text{m}$  long wire of gold that also connected two macroscopic, gold contact pads. The electrical contact pads were prepared by "stamping" the surface of a gold film using  $\text{CH}_3(\text{CH}_2)_{15}\text{SH}$  as an "ink".<sup>20</sup> We used a block of poly(dimethylsiloxane) (PDMS) that contained a 10- $\mu\text{m}$ -wide groove in its surface as the stamp. The groove was prepared by searing the surface of the PDMS with the hot (glowing red) blade of a surgical scalpel (Figure 2a,b). Micromachining of the gold wires was performed using the cut end of a carbon fiber with a diameter of 10  $\mu\text{m}$  (see Figure 3a-c). The resistance of the wire shown in Figure 4c,d was measured to be  $360 \pm 10 \Omega$ , and the corresponding resistivity of gold in the wire was estimated, using eq 1 to be  $12 \times 10^{-6} \Omega \text{ cm}$ . To confirm that the measured resistance was due to the wire, we severed the wire using a diamond microtome that was mounted under an optical microscope. The electrical resistance between the two contact pads after the wire was severed was measured to be  $>20 \text{ M}\Omega$ . The estimated electrical resistivity of gold in the 200 nm wide  $\times$  25 nm thick  $\times$  15  $\mu\text{m}$  long wire ( $12 \times 10^{-6} \Omega \text{ cm}$ ) was higher by a factor of 5 than that of bulk gold ( $2.44 \times 10^{-6} \Omega \text{ cm}$ ). This difference, again, is probably caused by constrictions in the cross-sectional area of the wire as a result of micromachining.

Micromachining, in combination with molecular self-assembly and wet chemical etching, can be used to fabricate multiple, closely spaced ( $\leq 1 \mu\text{m}$ ) microstructures of gold. Figure 5a,b show parallel,  $\sim 0.5\text{-}\mu\text{m}$ -wide wires of gold separated from each other by  $\sim 1 \mu\text{m}$ . The structures were prepared from a 100-nm-thick film of gold using the tip of a surgical scalpel blade as the machining tool. These closely spaced structures are formed, we believe, from the raised edges of micromachined grooves that extended through the thickness of the gold film to, or near to, the underlying glass (or silicon) substrate (see Figure 6). The fabrication of these structures was, in the first instance, accidental. We found, however, that these structures could be prepared routinely by machining with large loads ( $>10 \text{ mN}$ ) applied to the tip of a scalpel blade or by using thin films of gold.

Figure 7 shows collinear, 1- $\mu\text{m}$ -wide,  $\sim 100\text{-nm}$ -thick wires of gold separated from each other by a 0.8- $\mu\text{m}$ -wide, electrically insulating gap (see below). The rough morphology of the surface of the wires and the pits in the centers of the wires probably result from etching of gold in areas that were not protected (defects) by the SAM of  $\text{CH}_3(\text{CH}_2)_{15}\text{S}$ . The gap in the wire was fabricated by machining perpendicular to the wire using the tip of a scalpel blade. Prior to making the gap, the electrical resistance of the continuous wire was 4400  $\Omega$ ; after machining the gap, the resistance was measured to be  $>200 \text{ M}\Omega$ . We have used structures of the type shown in Figure 7 as working electrodes and counterelectrodes of an electrochemical cell.<sup>21</sup>

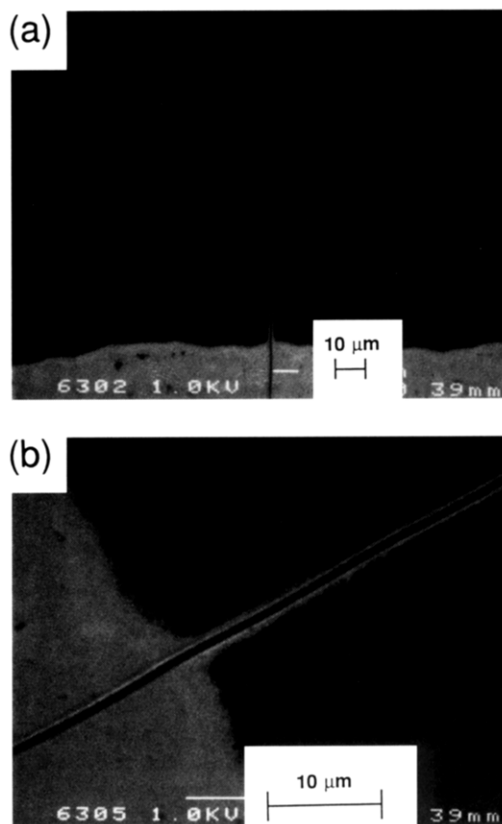


**Figure 5.** Scanning electron micrographs of parallel wires of gold (top views): (a) and (b) show  $\sim 0.5\text{-}\mu\text{m}$ -wide wires of gold separated from each other by  $\sim 1 \mu\text{m}$ . The wires were prepared from 100-nm-thick gold supported on glass. The accelerating voltage was 1.0 kV to minimize charging of the glass substrate.

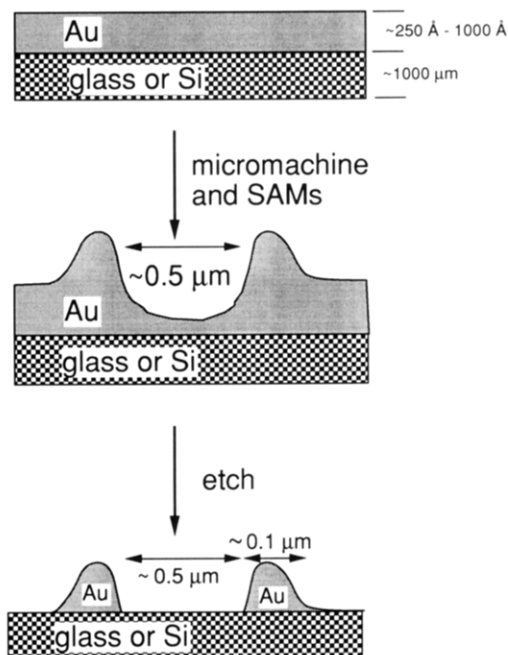


**Figure 6.** Schematic illustration of the processes leading to the formation of microstructures of the type shown in Figure 5. These closely spaced structures are formed, we believe, from raised edges of micromachined grooves.

Microstructures of the type shown in Figure 4 were used as masks for the wet etching of silicon. Figure 8 shows SEMs of a multilayer structure of silicon and gold that was fabricated using a 1- $\mu\text{m}$ -wide, 100-nm-thick wire of gold as a mask for an anisotropic etchant of silicon (30

(19) *Handbook of Chemistry and Physics*, 65th ed.; CRC Press: New York, 1985; p F-118.

(20) Kumar, A.; Whitesides, G. M. *Appl. Phys. Lett.* **1993**, *63*, 2002.

(21) Abbott, N. L.; Whitesides, G. M.; Rolison, D. R. *Langmuir*, in press.

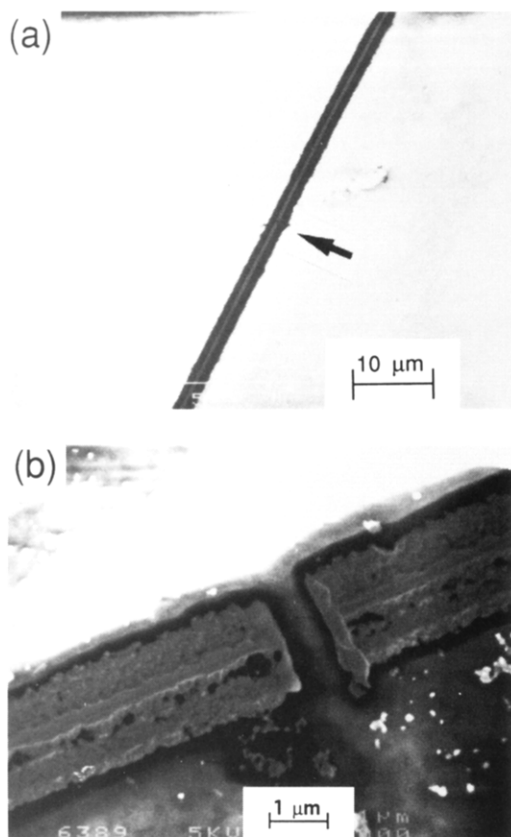


**Figure 7.** Scanning electron micrographs of collinear, 1- $\mu\text{m}$ -wide, 100-nm-thick wires of gold separated by a 0.8- $\mu\text{m}$ -wide electrically insulating gap: (a) low magnification, top view. The gap is indicated by an arrow. (b) High magnification image of the gap. The gap appears to be free of gold. The pits in the centers of the wires were probably produced during the wet etching of gold (see text for details). The accelerating voltage was 5.0 kV; the bright areas on the image were caused by the charging of the glass substrate. The dark halo that surrounds the gold wires is caused, we believe, by the wire acting as a collector of secondary electrons.

min in 2 M KOH in water/isopropyl alcohol at 45 °C.<sup>22</sup> The sample was prepared for imaging by fracturing the silicon wafer perpendicular to the longitudinal axis of the multilayer structure. The sides of the silicon ridge are Si(111) and form an angle of  $\sim 125^\circ$  with the top surface of the structure [Si(100)]. The gold wire caps the (100) crystallographic face of the silicon. The center of the gold mask, which directly contacts the underlying silicon, appears darker than its edges. The edges of the gold wire appear to protrude beyond the silicon structure. After 200 min of etching, the gold was displaced from the Si(100) surface.<sup>23</sup> The width of the silicon ridge was  $\sim 10 \mu\text{m}$ , which was greater, by a factor of 10, than the width of the gold mask from which the structure was fabricated. We believe that during the 200 min of etching, attrition of the Si(111) faces was sufficient to undercut the gold mask.

### Conclusions

We have demonstrated that micromachining, molecular self-assembly and wet chemical etching can be used to

(22) Aqueous solutions of KOH and isopropyl alcohol are an anisotropic etchant of silicon. The (111) crystallographic plane of Si is more closely packed than the (100) plane and, therefore, the (111) plane etches at a slower rate than the (100) plane.<sup>7</sup>

(23) The gold wire was displaced from the surface of the silicon during etching and was found floating in the bath of etching solution.

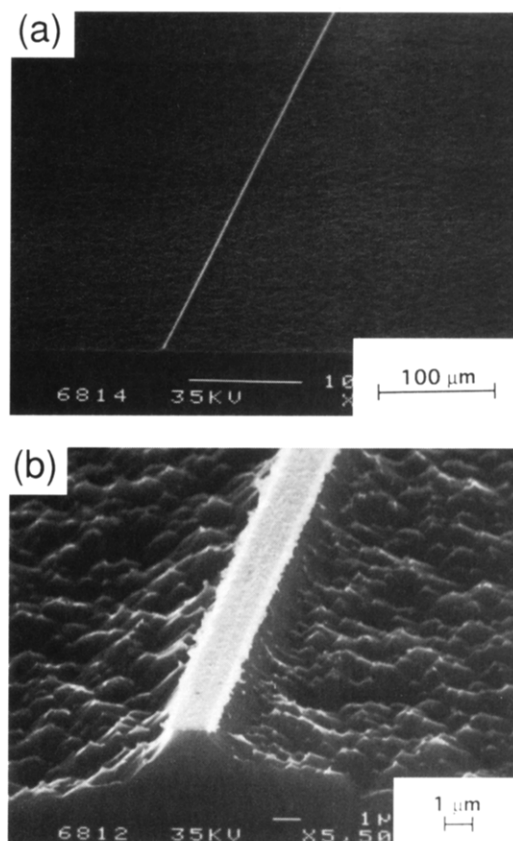


**Figure 8.** Scanning electron micrographs of heterostructures of silicon and gold prepared using 1- $\mu\text{m}$ -wide wires of gold as masks for an anisotropic etch of silicon (2 M KOH in water, 20% isopropyl alcohol at 45 °C):<sup>22</sup> (a) and (b) show cross-sectional images of a structure that was fabricated by etching for 30 min. The gold wire caps the top surface of the silicon ridge: the Si(100) crystallographic face. The sides of ridge are Si(111). The sample was tilted 60° from the horizontal for imaging.

fabricate microstructures of gold supported on silicon or glass substrates. Simple methods of micromachining were used to fabricate electrically conducting wires of gold with cross sections as small as  $200 \text{ nm} \times 25 \text{ nm}$ . Microstructures with more complex geometries and parallel and collinear wires separated by  $<1 \mu\text{m}$  were also fabricated. These gold microstructures served as masks for the etching of silicon to fabricate multilayer structures of gold and silicon with micrometer-scale dimensions. The procedure reported for the preparation of these structures is a simple one that uses commercially available chemicals and does not require a large investment in laboratory equipment. These features make this methodology a useful one for laboratories that do not have access to electron-beam and photolithographic facilities and for fabrication problems in which lithography may be impractical: on interior or curved surfaces; for customized structures; with radiation-sensitive substrates. It also suggests that micromachining of SAMs on soft, deformable substrates may be a general route to certain types of closely spaced microstructures. This procedure, we believe, can be scaled to dimensions  $<10 \text{ nm}$  by using STM and AFM to micromachine SAMs formed on the surface of metal films.

### Experimental Section

**Materials.** Titanium (99.999+%), Au (99.999+%), and  $\text{CH}_3(\text{CH}_2)_{15}\text{SH}$  and were obtained from Aldrich.  $\text{HO}(\text{CH}_2)_2\text{SH}$  was obtained from Bio-Rad Laboratories. KOH and KCN was

obtained from Fisher Scientific. Surgical scalpel blades were purchased from Feather Industries (Tokyo) and carbon fibers (diameter 10  $\mu\text{m}$ ) from Hyperion (Massachusetts). Polished Si(100) wafers were obtained from Silicon Sense (New Hampshire).

**Preparation of Gold Films.** Glass microscope slides (VWR Company) were cleaned in piranha solution (30%  $\text{H}_2\text{O}_2$  and 70%  $\text{H}_2\text{SO}_4$ ). **Warning: Piranha solution should be handled with caution; in some circumstances (most probably when it had been mixed with significant quantities of an oxidizable organic material), it has detonated unexpectedly.** The slides were rinsed with distilled water and dried in an oven prior to placement in the evaporation chamber. Titanium ( $\sim 6 \text{ \AA}$ ) was evaporated at 1  $\text{\AA}/\text{s}$ , and gold (1000 or 250  $\text{\AA}$ ) was evaporated at 5  $\text{\AA}/\text{s}$  onto clean glass microscope slides in a cryogenically pumped chamber (base pressure  $\approx 8 \times 10^{-8}$  Torr; operating pressure  $\approx 1 \times 10^{-6}$  Torr) using an electron beam. The resulting gold films are polycrystalline but have a predominant crystallographic orientation that is (111).

**Preparation of Microstructures of Gold.** Films of gold (250 or 1000  $\text{\AA}$  in thickness) were immersed in an ethanolic solution of  $\text{HO}(\text{CH}_2)_2\text{SH}$  ( $\sim 100 \text{ mM}$ ) for 10 min. Regions of bare gold were prepared by micromachining the monolayer of  $\text{HO}(\text{CH}_2)_2\text{S}$  to expose the underlying gold. Details of the micromachining are described in the text. Self-assembled monolayers of  $\text{CH}_3(\text{CH}_2)_{15}\text{S}$  were formed selectively on the micromachined regions of bare gold by immersing the sample in an ethanolic solution of 100 mM  $\text{CH}_3(\text{CH}_2)_{15}\text{SH}$  for 10 s. After immersion in the solution of  $\text{CH}_3(\text{CH}_2)_{15}\text{SH}$ , the sample was washed in heptane rather than ethanol. Washing in ethanol resulted in a waxy residue on the surface of the gold and incomplete etching of the areas of the gold film covered with

$\text{HO}(\text{CH}_2)_2\text{S}$ . Regions of the gold film covered with  $\text{HO}(\text{CH}_2)_2\text{S}$  were selectively etched by immersing the entire gold film in an aqueous solution of 1 M KOH and 0.1 M KCN that was sparged with  $\text{O}_2$  and vigorously stirred. The 250- $\text{\AA}$ -thick films of gold supporting monolayers of  $\text{HO}(\text{CH}_2)_2\text{S}$  etched in 5–10 min, and the 1000- $\text{\AA}$ -thick gold films etched in  $\sim 45$ –60 min.

**Conductivity Measurements.** Macroscopic electrical contact pads were prepared by dipping both ends of the gold film in neat hexadecanethiol for 20 s. A  $\sim 15$ -mm region of bare gold was left in the middle of the gold film. The wires were prepared on this region of bare gold. Conductivity measurements were performed with a four-point conductivity meter using osmium probes (spacing 1.6 mm; radii 0.13 mm).

**Etching of Silicon.** Wafers of Si(100) were masked with wires of gold using the procedure described above. Before the wafers were etched in a solution of 100 mL of 2 M KOH and 25 mL of isopropyl alcohol, the oxide layer was removed from the wafers by dipping them in 10% HF. The aqueous solution of KOH and isopropyl alcohol was stirred vigorously and thermostated at 45  $^\circ\text{C}$  during the etching of the wafers.

**Acknowledgment.** This research was supported in part by the Office of Naval Research and the Advanced Projects Research Agency. Electron microscopy was performed using facilities of the Materials Research Laboratory at Harvard University. The authors wish to thank Hans Biebuyck, Steven Bergens, and Watson Lees for insightful discussions. John Folkers and Paul DiMilla are thanked for their technical assistance.